The photophysics of solution processable semiconductors for applications in optoelectronic devices

Abdu-Aguye, Mustapha

DOI:
10.33612/diss.111696164

Chapter 1

This chapter is devoted to a general introduction to solar energy, to the photophysics of solar energy relevant semiconductors, and the motivation for the project. Since this thesis deals with different semiconductors using a few different techniques for investigations in different chapters; to enhance the readability of the text and to avoid overly long introductory texts in every chapter, a general (non-exhaustive) overview of the materials and important methods that will be covered in later parts of this thesis is provided. Finally, a short section is dedicated to the outline of the later chapters.

1.1 Introduction

In more ways than one, the sun is central to our existence. It is the primary source of the heat and light necessary for life: it is responsible for the so-called "*Goldilocks Zone*" our planet occupies in the solar system; it also powers photosynthesis enabling plants (and other living organisms) to create chemical energy and oxygen from elemental nutrients, natural pigments, and carbon dioxide. All ingredients which were created in the immediate aftermath of the big bang. Not to mention the role it plays in the earth's orbit – which has as consequence many physical phenomena in our planet. Unlike most other sources of energy, solar energy is abundant, sustainable and relatively well distributed around the earth – attributes which make it extremely desirable as one (of ideally, many) sources of energy to be exploited to further our advancement as a species.

Global demand for energy (and in particular, electricity) is on the increase. This is due to several factors: the first is that the global population has continued to rise steadily. The second is that the pace of industrial and technological advancement has concurrently grown leading to an increase in wealth which has, in turn, changed our lifestyles from basic survival needs (food, hygiene) to more technologically advanced ones (transportation, communication, electronic devices, data handling and storage, etc.). There have of course been continuous advances in energy efficiency, generation, transmission, and use, but they simply have not kept pace with the increase in demand. Today, the bulk of our energy consumption (over 90% at the end of 2017, see Figure 1.1) is supplied by burning fossil fuels like petroleum, gas, and coal which are non-renewable sources of energy. Our continued reliance on fossil fuels has several drawbacks – chief of which are the finiteness of their availability and the damage/pollution they cause to the environment during exploration and combustion.

Over the past two decades, the global community has identified matters relating to energy (production, accessibility, and efficiency) as being important aspects towards achieving inclusive and sustainable development as well as to the continued habitability of our planet. One question that is continuously being debated is: "*How do we continue to meet global targets for inclusive and sustainable development without causing major, irreversible damage to the planet for future generations?*". This extremely important question is reflected in several recent initiatives such as the United Nations' sustainable development goals[1] (SDGs) and the Paris climate accords[2] to allay the effects of climate change. One major agreement is to limit the average global

temperature increase to 2 ºC by sharply reducing global CO_2 emissions. To achieve this, part of the focus has been on adding renewable and sustainable energy sources to meet our current and future needs. From all indications[3], there is still clearly much work to be done in this regard.

Revisiting the issue of electricity demand, production and use; it is worth mentioning two important developments that have been strong drivers of demand for non-industrial purposes. The former is the electrification of energy use, and the latter, is the development and proliferation of electronic devices, most especially those utilising semiconductor and/or photonic technologies.

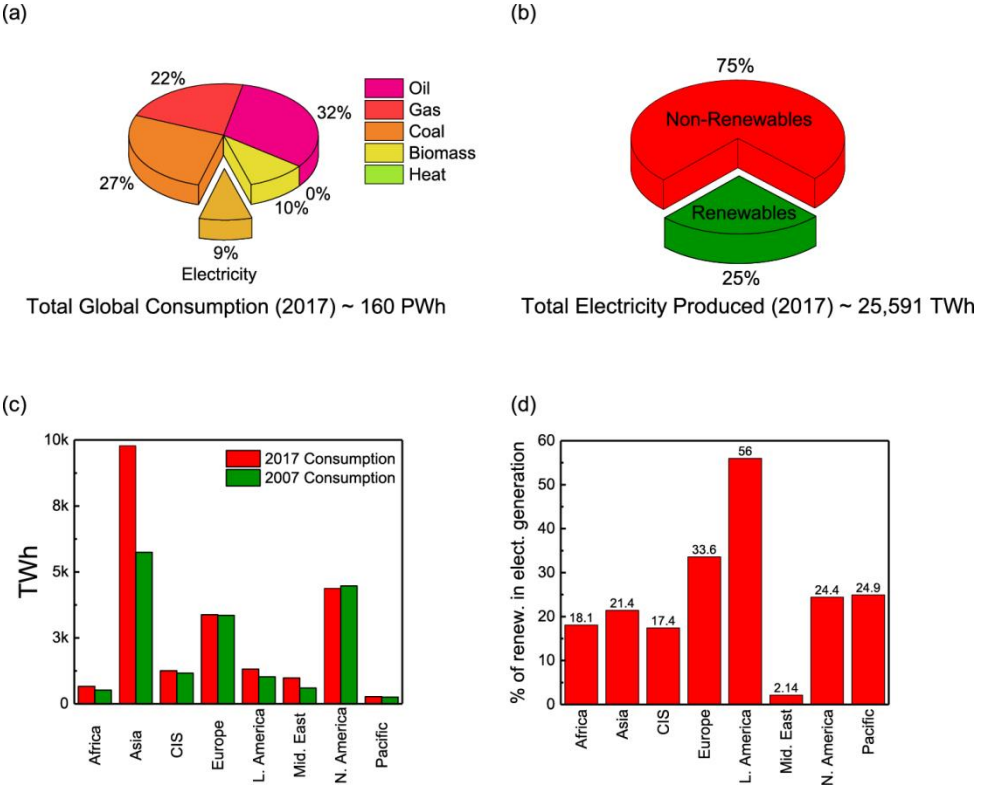

Figure 1.1: (a & b) Global energy consumption and the share of renewables in electricity generation for 2017; (c) our demand for energy has grown over the past decade; (d) although renewable sources are now being added to the generation sources, there is still more work to be done in this regard. (Source: Global Energy Statistical Yearbook[3])

This increase in demand, viewed together with the scarcity of resources (fossil fuels are non-renewable) and the severe environment impact their exploration and

combustion cause are a compelling justification for why scientists and engineers have been strongly motivated to research and develop alternative energy sources. Solar technologies are one of several renewable energy technologies to garner attention as a sustainable, well-distributed and environmentally friendly means to meet current (and future) electricity demands.

1.2 Solar Cells

A solar cell (or photovoltaic cell) is a device that creates electrical power upon absorption of light; i.e. it converts energy in the form of light to electricity via the photovoltaic effect. Solar cells are made from Semiconductors such as Silicon, Cadmium Telluride etc. The market for solar cells has traditionally been dominated by silicon solar cells[4]. This is due to several reasons such as its' abundant occurrence, and the decades long head start that it has had in the photovoltaics field. However, since the early 90s, several new material systems have emerged, whose rapid progression now challenge the dominance of silicon as the premier photovoltaic (PV) material – examples of these *emerging* materials (and their technologies which are termed "3rd Generation") and their progress relative to silicon as solar cells in the past decade are illustrated in Figure 1.2 below.

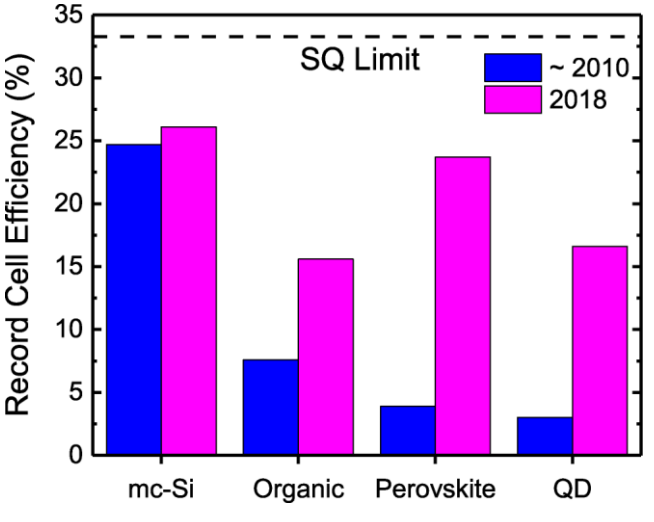

Figure 1.2: Record research cell efficiencies for the materials studied in this thesis versus monocrystalline silicon compared between approximately 2010 to date. Source: NREL research cell efficiency chart[47].

In the simplest architecture, a solar cell consists of an active layer composed of a semiconductor, placed between two electrodes - one of which must be transparent

to allow light to pass through to be absorbed by the active layer. It is also common to have additional functional layers to improve the extraction of either electrons or holes (charge extraction layers), for improved electrical performance (electron or hole blocking layers/selective electrodes) or to improve light management (anti-reflection coatings). A discussion of solar cell device characterisation and an illustration of the architecture of a typical solar cell is depicted in later in this chapter – in section 1.7.3.

The Shockley-Queisser (SQ) limit, which sets the maximum efficiency of a single absorber layer with an ideal bandgap for a solar cell at approximately 33%[5]. This number is based on a detailed balance between loss of photons with energy below the bandgap, thermal losses induced by photons with energy above the bandgap, blackbody radiation, and radiative losses. Balancing the trade-off between the former two losses – an ideal bandgap of 1.3 eV is obtained under standard conditions. In Figure 1.2, the modest improvement of Silicon over the period 2010-2018 is partially motivated by its indirect bandgap of 1.1 eV and practical limitations in devices such as cell resistance, interconnects etc.

Initially, these emerging PV materials were considered to be direct challengers to the prominence of silicon; whose production is comparatively costly and energy intensive due to their desirable material properties. For instance, organic semiconductors, hybrid perovskites and colloidal quantum dots; which are characterised by direct band gaps, high absorption coefficients, large colour tuneability, solution processability etc. However, improvements in manufacturing techniques and the economics of (large) scale production has continuously driven down the levelised cost of silicon PV well below 1 USD per kilowatt hour ($/kWh) – a number considered to be the threshold for mass commercialisation and widespread adoption[1]. These emerging materials, despite meeting the promise of being cheaper to produce from a materials point-of-view still suffer from low efficiency (compared to silicon), stability (operational lifetime) and high associated costs (such as investments necessary for optimised mass production). They have therefore suffered limited commercial success beyond lab-scale devices.

As research into workable solutions for the aforementioned challenges continues, there seems to be a gradual pivot towards leveraging the inherent advantages these emerging material systems have over silicon; namely, their extremely high

[1] This is likely due to a comparison with the levelised costs of other power generation sources.

absorption coefficients, their mechanical properties and ranges of bandgaps which enable them to be made into ultrathin conformal layers of various colours on different kinds of supports; which opens avenues for use in disposable and flexible electronics; and also in cases where aesthetics are important (architecture, art installations, etc.). An associated advantage of these materials is the high energy density (per Kilogram) possessed by these material systems which makes them ideal for cases where lightweight solutions are more important than cost (for instance, in satellites & space exploration). A final (possible) niche for these emerging material systems leverages their band gap tunability as either front- or rear-sub cells in tandem architectures together with silicon to hopefully move beyond the SQ limit.

The materials reported in this thesis - namely (organic) semiconductors, hybrid perovskites and colloidal quantum dots fall into the solution-processable subclass of these emerging material systems. In the applications discussed, they are generally used in thin films (with thicknesses between ~150nm and 500nm). The section below gives a brief overview of each material class and their physical properties; these properties, as can be imagined, have important implications in how they are processed, characterised and utilised in devices.

1.3 Solution Processable Semiconductors

All the semiconductors studied in this thesis are solution-processable; meaning that in all characterisations and devices, the material is dissolved in a suitable solvent to make a solution (or ink). These solutions (or inks) can then be used to deposit thin films via a host of techniques such as spin-coating and blade-coating – these techniques are generally suitable for films of thicknesses from the nanometres to the micron range, respectively. Depending on the specific material, solution-processability is either imparted during synthesis via side-chains in organic semiconductors, ligands in semiconducting quantum dots (QDs)or as a consequence of the solubility of precursors in the case of hybrid perovskites. Further details of the materials used in this thesis is provided in the following sections.

1.4 Polymers

A polymer is a large molecule, which essentially consists of multiple repeating units of a smaller molecule, called a monomer, created by a process referred to (unsurprisingly) as polymerisation. Polymers are extremely ubiquitous in nature, ranging from naturally occurring macromolecules such as DNA, cellulose, and proteins to synthetic materials important for our everyday lives such as polyethylene terephthalate (PET), polyacrylates & polyesters used in water bottles, cosmetics and textiles. The generic term "plastic" is used to refer to polymeric materials and derivatives thereof – referring mostly to their mechanical properties.

Due to their ubiquity, classification of polymers varies depending on scale, physical basis as well as functionality[6]. Therefore, different kinds of polymers can be discussed depending on their structure and electronic properties.

1.4.1 Semiconducting Polymers

(Semi)conducting polymers became popular in the 1980's after the discovery of conductive polyacetylene by Shirakawa, Heeger and MacDiarmid[7] – which eventually led to their being awarded the Nobel Prize in Chemistry in 2000[8]; although there had been an earlier report on the redox properties of other types of polymers[9] . The former sparked off decades of research and collaboration between fields of chemistry and physics. During this time, many concepts from semiconductor physics were used to understand the properties of this new class of semiconductors (also called organic semiconductors), which later developed into a distinct language for describing the properties of these materials.

Polymers are considered to be *organic* materials; the term "*organic*" is used in the sense that they are composed almost entirely of carbon (C) and hydrogen (H) atoms. Although in some common semiconducting polymers, other atoms such as oxygen (O), nitrogen (N) sulphur (S), silicon (Si) etc. occasionally feature and are referred to as heteroatoms. In order to discuss the properties of polymers relevant to this thesis, it is necessary to first address the molecular origins of the optical and electronic properties of semiconducting polymers.

Carbon, belongs to group 4 of the periodic table – meaning that it contains 4 outer electrons and usually forms covalent bonds with other atoms to form molecules. When Carbon atoms form bonds, orbital hybridisation occurs; which is a process whereby atomic orbitals in atoms undergoing bonding mix to form hybrid

molecular orbitals (MOs) with distinct characteristics from their parent atomic orbitals to enable bonding occur. In particular, Carbon can form *sp*, sp^2 or sp^3 hybrid orbitals from one *s*-orbital and one, two or three *p*-orbitals respectively. Organic semiconductors usually consist of alternating single and double bonds, forming a pi-conjugated system with a planar backbone formed from sp^2-hybridised Carbon atoms (called sigma bonds) and partially occupied p_z-orbitals perpendicular to the sigma bonds, called pi-bonds. Electrons in pi-orbitals ("pi electrons") in pi-conjugated systems are responsible for many of their optical and electronic properties owing to their delocalised nature [10].

In semiconductor physics, a very important concept is the bandgap, which represents the difference (in energy) between the (top of the) valence- and (bottom of the) conduction- bands of a semiconductor. (Frontier) MO theory[11,12] allows us translate this concept into the language of organic materials via the idea of "frontier orbitals" – which are the highest occupied molecular orbital (termed HOMO) and the lowest unoccupied molecular orbital (LUMO) of a molecule; which are analogous in certain sense, considering the discrete nature of them, respectively to the valence and conduction levels. We can take this further, by using the HOMO-LUMO gap as an ideological analogue to a bandgap in organic materials. When an electron in a MO is suitably excited, by for example, absorption of a photon – it can move up to an unoccupied MO at higher energy; the lowest possible such transition therefore is from the HOMO to the LUMO. Although organic semiconductors can be referred to as either *n*- or *p*- type, an important distinction from inorganic semiconductors where this designation have to do with doping is that in the former case, it means that they are either electron-transporting materials or hole transporting materials, respectively.

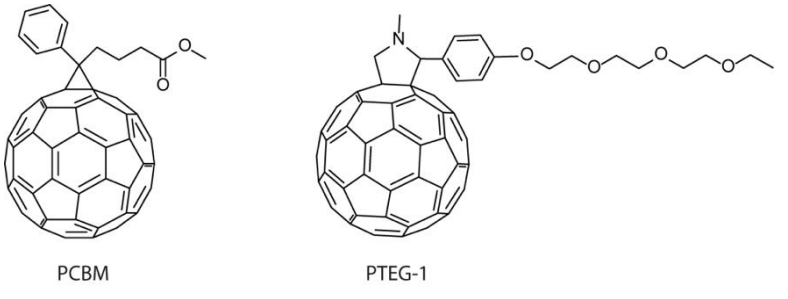

Figure 1.3: Chemical structure of the two (main) fullerene derivatives that feature in this thesis: PCBM and PTEG.

A different but related class of organic semiconductors are organic molecules (which are sometimes called "small molecules"); these molecules are often either unpolymerized or *oligomerized, i.e.,* they contain only a few repeating units of a monomer. Small molecules generally also contain sp^2-hybridised Carbon atoms which give them similar optical and electronic properties to polymers. In this thesis, the main small molecules that features are the fullerene derivatives: phenyl-C_{61}-butyric methyl acid ester (PCBM) and 2'-[4"-((((2-ethoxy)-2-ethoxy)-2-ethoxy)-2-ethoxy)phenyl]-fulleropyrrolidine (PTEG-1); which are both *n*-type organic semiconductors used as electron acceptors in organic and hybrid solar cells (shown in Figure 1.3). Among the several properties of organic semiconductors, those most relevant to this thesis are related to their interaction with light (absorption and emission) and the properties that derive from their excited state dynamics[13].

One of these properties is their excitonic nature – because organic semiconductors have an intrinsically low dielectric constant (typically between 2 ~ 4) as a consequence of being composed of species bound by relatively weak *van der Waals* forces when in thin film or crystals. When they are excited they form strongly bound, correlated electron-hole pairs (*Frenkel* excitons) which require (additional) energy of the order of 0.3 – 0.5 eV to be split into free charges[14]. This (binding) energy is generally much larger than the available thermal energy (given by k_BT at room temperature ≈ 25.6 meV) and thus necessitates the use of a so-called type-II heterojunction (*bulk-heterojunction)* to facilitate charge separation for example in a solar cell[15–17].

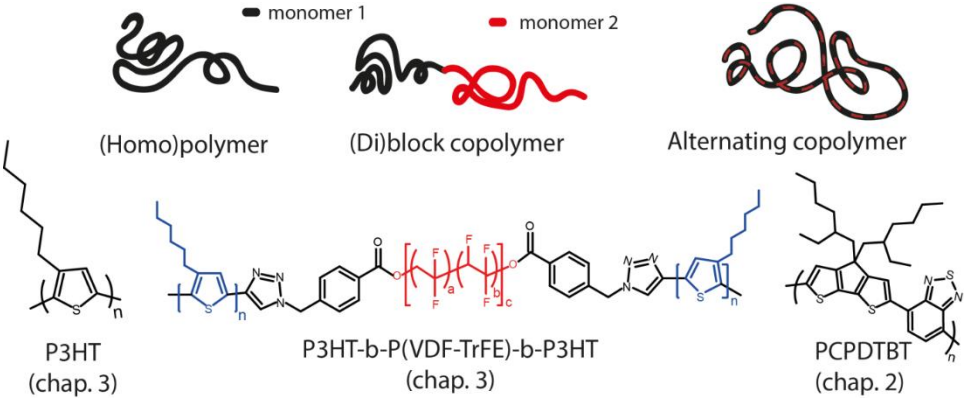

Figure 1.4: Schematic representation of the types of polymers featured in this thesis and corresponding chemical structures and acronyms of examples of each type. Full names are in the respective chapters.

A bulk-heterojunction is a blend of two semiconductors (a donor and acceptor, or *p*- and *n*- type molecules) which are assembled into an interpenetrating network with domains on the order of 10s of nanometres. Upon photoexcitation, the donor forms excitons which then diffuse until they encounter an interface with an acceptor; whose large electron affinity provides the driving force for exciton dissociation, enabling the formation of free charges - eventually to be collected by the electrodes. The formation of free charges is generally preceded by the formation of a *charge transfer* (CT) state[18,19] wherein the exciton (a CT exciton) is delocalised between adjacent the donor and acceptor molecules. Bulk heterojunctions have a much higher D-A interfacial area compared to simple D-A bilayers which make them more efficient compared to bilayer-based devices. Worth noting also is that while many organic semiconductors can (and often do) possess some nanoscale or even supramolecular order when in solid state (depending on several factors).

A result of being solution processable is inevitably that structural imperfections in nanoscale order (defects) and impurities are commonplace; these in turn affect the transport properties and lead to a distribution of localized electronic states in these kinds of semiconductors. This phenomenon results in organics being *disordered semiconductors*; and transport through them treated as discrete hops between localized transport sites[20].

Broadly speaking, most research into polymer optoelectronics utilise either homo-polymers or alternating donor-acceptor (D-A) type copolymers. The former are composed of a single type of monomer; and the latter are composed of more than one monomer. D-A copolymers are the result of research into developing polymers with narrow-bandgaps (compared to most homo-polymers) – which as a consequence are able to absorb more of the solar irradiance spectrum; and therefore to yield higher power conversion efficiency in organic photovoltaics (OPVs). Figure 1.4 shows the polymers that feature in this thesis.

1.4.2 Ferroelectric Polymers

Next to semiconducting polymers, another interesting and technologically relevant sub-class of polymers are ferroelectric polymers. Ferroelectricity is closely linked to other properties such as piezoelectricity and pyroelectricity[21]. That is, the genesis of ferroelectricity is linked to having a polar crystal class which, being non-centrosymmetric, leads to polarization that can be oriented by means of external

effects such as mechanical stress (for piezoelectric materials) or temperature (for pyroelectric materials). Therefore, a characteristic ferroelectric polarization hysteresis loop can be obtained by plotting the polarization versus the applied electric field. Initially, the main ferroelectric materials were (inorganic) ceramics such as lead zirconate titanate (PZT), barium titanate and quartz – which while seemingly have higher piezo- and pyro- electric coefficients still yield comparable electromechanical coupling strengths to ferroelectric polymers due to their relatively lower dielectric constants and excellent mechanical properties[22].

The workhorse for the study of such polymers over the past few decades has been Polyvinylidene difluoride (commonly called PVDF) and more recently, several related copolymers such as poly(vinylidene difluoride trifluoroethylene), or P(VDF-TrFE). These polymers contain polar Carbon-Fluorine bonds in their constituent monomers; and crystallize in a manner which enables the dipoles to remain aligned; therefore, maintaining a polarization. While this is a generally accepted explanation for their physical properties the details of their operation in several kinds of devices are still under debate[23–25]. Other than their main use in electromechanical transducers, they have successfully been utilised in other applications such as gate electrodes in FETs, components of polymer blends for resistive memories, batteries and also in organic solar cells[26–28].

1.5 Semiconducting Nanocrystals, Or Quantum Dots

A quantum dot (QD) is a fragment of a semiconductor containing hundreds to thousands of atoms with the bulk bonding geometry and surface states eliminated by enclosure in either a larger bandgap material or with molecular ligands[29]. Quantum dots exhibit both electronic and optical properties that are strongly size dependent – a consequence their dimensions being less than the exciton Bohr radius of the excitons in the bulk material: a situation commonly called the *quantum confinement* effect, as charge carriers in the QD are *quantum confined*[30].

These size-dependent properties of QDs can further be understood in terms of the particle-in-a-box formalism in quantum mechanics, where a particle in a confined potential (box) has only certain allowed energy levels, E (or *Eigenvalues*), indexed by integers n, which can be obtained by solving the *Schrödinger* equation[31]. This implies that the energy level spacing, ΔE, increases when the size of the QD decreases. In more concrete terms, the bandgap, E_g, of a QD with radius r, can be written in

terms of the bandgap of the bulk semiconductor E_0 and a "confinement energy"; as a first approximation it is given by the phenomenological equation:

$$E_g \approx E_0 + \frac{\hbar^2 \pi^2 (m_e + m_h)}{2r^2 m_e m_h} \qquad (1.1)$$

Where m_e and m_h are the effective masses of electrons and holes in the QD respectively. This allows a range of colours from the ultraviolet (UV) to the (near) infrared (NIR) spectral regions to be obtained from the same material by simply changing the size of the QD, famously seen in CdSe QDs. Furthermore, many QDs have excellent absorption coefficients and tunable carrier mobilities – making them strong candidates for thin film electronics.

In recent years, colloidal QDs (CQDs) obtained by wet-chemical methods have progressed to the point where knowledge of synthetic techniques yields excellent scale and size-selectivity for many important types of QDs for optoelectronic applications such as lead- and cadmium- chalcogenides, as well as indium- and gallium-based QDs. The main power of CQDs after their size-dependent properties lies in the possibility of obtaining large amounts from earth abundant materials (at relatively low cost); which can then be assembled into arrays or assemblies, referred to as QD solids, using already well-known techniques for mass production of thin films such as blade-coating. As-synthesized CQDs are often capped with long aliphatic ligands (such as oleic acid) which provide colloidal stability but also form an insulating barrier which prevents charge transport between adjacent QDs; this is why QD solids for device applications are assembled with shorter ligands which allow charge transport by tunnelling between individual QDs in an array. Until a few years ago, the rise of CQDs in photovoltaics has generally been led by lead sulphide (PbS)-based QDs[32]. This can be attributed to its' large exciton Bohr radius (enabling the synthesis of larger QDs without losing confinement) and relatively narrow bandgap (~ 0.4 eV in the bulk) which enable absorption up to the infrared coupled with advances in our understanding of its' fundamental properties, synthetic methodologies, surface passivation, and device engineering[33].

Once QDs are brought into close proximity, charge transport becomes possible due to overlap of the electronic wavefunctions on adjacent QDs. Thus, a binding energy, β, can be used to approximate the coupling between QDs which is directly proportional to the probability that electrons can tunnel from one QD to another[34]

$$\beta = h\Gamma \propto exp\left(-2\Delta x\sqrt{\frac{2m^*}{\hbar^2}\Delta E}\right) \qquad (1.2)$$

Where ($\hbar$)h, m^*, Δx, and ΔE respectively represent the (reduced) Planck constant, the carrier effective mass, and the width and height of the energy barrier between adjacent QDs. This necessarily implies that the degree of coupling between QDs in an array is influenced by the ligands with which they are capped as well as the nature of their environment (*i.e.* the matrix around them). Other important practical considerations to make regarding PbS QDs are (i) surface stoichiometry, adsorbates and capping ligands can cause a shift in their Fermi energy (E_F) leading to a more pronounced *n*- or *p*- type behaviour[35]; and (ii) the incidence of crystal defects either during synthesis or subsequent to ligand exchange can enable the formation of sub bandgap states which can act as traps for charge carriers or recombination centres[36], which are undesirable. Figure 1.5 shows a schematic representation of isolated and coupled QDs and a cartoon depicting the effect of proximity on transport through *mini bands*[37] which are formed when QDs are brought into proximity with each other.

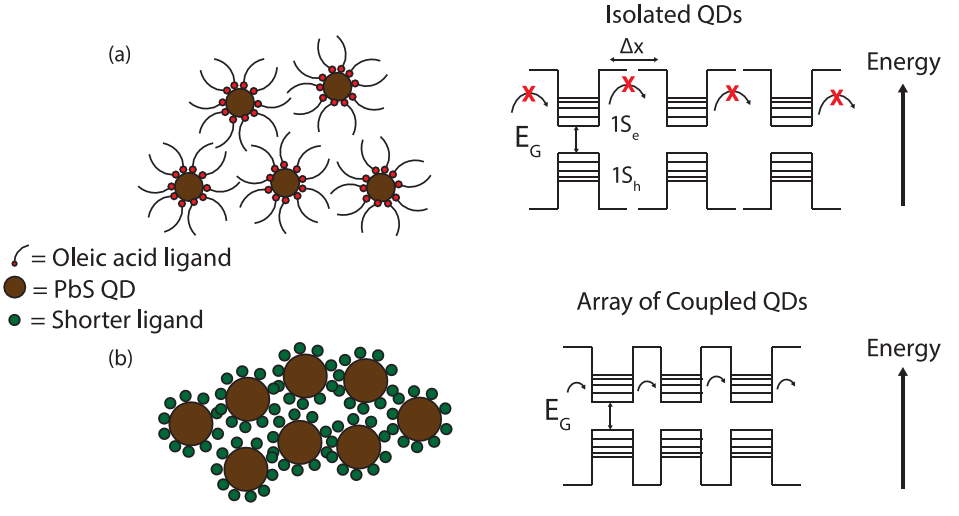

Figure 1.5: Schematic representation of PbS CQDs with either (a) oleic acid ligands or (b) shorter ligand which enables transport in the 'mini bands' formed. Figures on the right are a representation of energy levels between adjacent dots in both cases.

As mentioned earlier, as-synthesized CQDs are often capped with long aliphatic ligands for colloidal stability, and in order to facilitate transport in QD solids these ligands are exchanged with shorter ligands containing groups with high affinity for

the QD surface. The most common ligands used with PbS QDs include thiol compounds and amines such as 1,2-ethanedithiol (EDT), benzenethiol (BT) and benzenedithiols (BDTs), ethylenediamine (EDA) as well as 3-mercaptopropionic acid (MPA). Most recently, atomic passivation using halide ions from organo-halide salts such as tetrabutylammonium chloride, - iodide and -bromide have also been reported[38].

1.6 Hybrid Perovskites

Perovskites (named after Russian mineralogist *Lev Perovski*) are a class of materials that adopt the ABX_3 crystal structure of calcium titanate (see Figure 1.6); consisting of two cations of different sizes (*A* & *B*) and an anion (*X*). Structurally speaking, in the ideal cubic case – the *B* cation has six-fold coordination with the anion, *X*, forming a $[BX_6]$ octahedron[39]. In the extended crystal, the voids between these octahedra are filled with the *A* cations. In addition, when there is a large disparity between the sizes of the *A* & *B* ions, it can lead to buckling of the crystal and the formation of lower symmetry analogues (such as layered perovskites). The size requirement for stability is quantified by the *Goldschimdt* tolerance factor[40], α, which is expressed in terms of the ionic radius, *r*, of *A*, *B* and *X* as:

$$\alpha = \frac{r_A + r_X}{\sqrt{2}(r_B + r_X)} \qquad (1.3)$$

In the ideal cubic case, α falls between 0.9 and 1, but in many cases, when the *A* cation is small; orthorhombic and rhombohedral variants are formed, this usually occurs for $0.75 < \alpha < 0.9$. For applications in optoelectronics, early reports[41] on perovskites focussed on variants where the *A* cation was a small organic molecule (methyl-ammonium, *MA*) – hence the term "hybrid". Since that initial report, hybrid perovskites have grown unprecedentedly popular in the photovoltaic community with new applications still being reported almost weekly[2], an advantage they possess due being easy to synthesize[42], tolerant to defects[43,44], and to decades of research into other photovoltaic technologies.

A somewhat newer development are all-inorganic counterparts to hybrid perovskites featuring *A* cations such as caesium, rubidium and strontium – some of which have been demonstrated to be more thermally stable and to enable further engineering of the bandgap[45,46]. All these facts, coupled with advances in material

[2] The *Web of Science*™ citation index is an excellent way to check this assertion.

quality and device engineering have resulted in perovskites and perovskite-based materials holding a few certified record efficiencies in the emerging photovoltaic material category of the NREL efficiency chart[47].Figure 1.6 below shows the perovskite crystal structure.

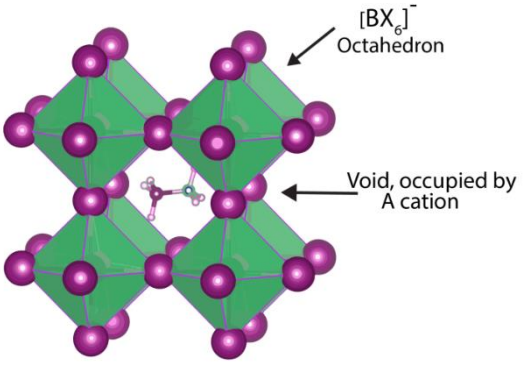

Figure 1.6: ABX_3 perovskite structure showing inorganic octahedra and the methyl ammonium cation contained within the voids. Figure adapted from Eames et al[62]

1.7 Methods

A few different experimental techniques have been applied to the materials studied in this thesis to understand various aspects of their optical and electronic properties and feature in almost every chapter. The section below gives a brief overview of such techniques and lays out examples of how measurements can be interpreted. A useful starting point for this is a discussion of concepts and methods related to elementary photophysical processes; and how these processes can be utilised to understand the properties of materials presented in this thesis.

When a semiconductor (or molecule) is in its' ground state S_0, it can interact with light, different phenomena can occur depending on the photon energy. One such phenomenon is that the energy of the photon is absorbed, resulting in a transition to an excited state S_1. This process can involve electronic and/or vibrational energy levels; in the former case – it is almost instantaneous due to the fact that electronic motions occur on much faster time scale than nuclear motions. For changes in vibrational levels during the electronic transition, the requirement is that the initial and final configuration of the molecule and its' surroundings (i.e. nuclear positions and momenta) be simultaneously compatible with each other - a rule formally called the *Franck-Condon* principle[48,49]. Within the higher vibrational levels of an excited state (say S_1) vibrational relaxation (called *internal conversion*) allows the molecule to "dump" the excess energy to its' surroundings non-radiatively, bringing it to the

lowest level of S_1. Once there, it can either undergo further internal conversion by coupling to another vibrational level of the lower ground state, S_0; or it can emit a photon (= fluoresce) and return to the ground state of S_0. A practical consequence of this is that provided that the system is excited above its' band gap, (most) fluorescence will be preferentially obtained from the lowest level of S_1; this is sometimes called the *Kasha-Vavilov* rule[50,51]. This radiative process enables us to perform photoluminescence spectroscopy to probe the excited states of emissive materials.

These concepts are nicely visualised in a simplified version of a *Jablonksi* diagram[52,53] shown in Figure 1.7. For clarity, transitions involving triplet energy levels have been omitted and only the vibrational levels of S_0, S_1 and S_2 are depicted.

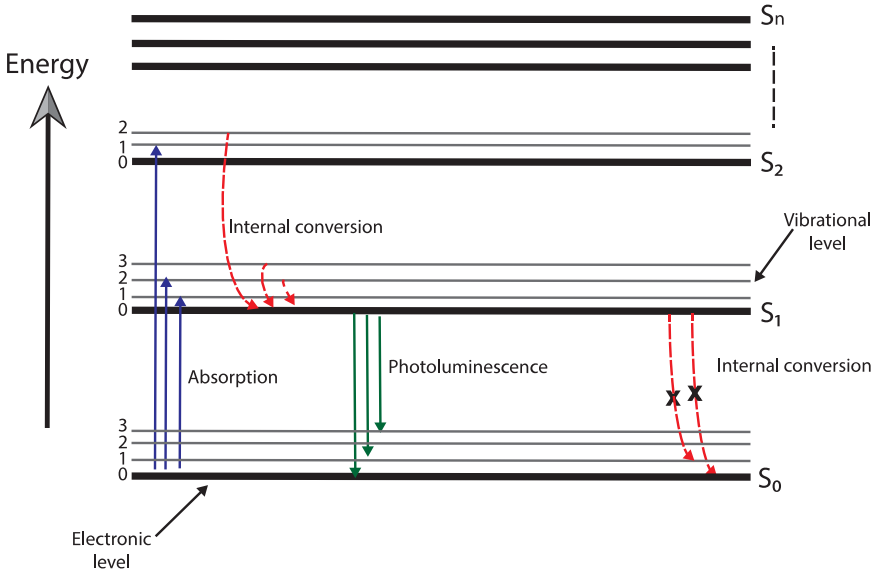

Figure 1.7: A simplified Jablonksi diagram showing the possible photophysical processes that can occur in a semiconductor.

1.7.1 Absorbance Spectroscopy

When a semiconductor interacts with light, it can be either reflected, absorbed, or transmitted. The former is related to the behaviour of light at the interface of two media and forms the basis of visual perception; whereas, the latter two are related quantities and can be intuitively understood as: *if all the light shone on a semiconductor*

passes through it, then transmittance is 100% and absorbance is 0; if on the other hand none of the light passes through, then transmittance is 0% and absorbance is infinite. Where the transmittance is the fraction of radiant power that passes through a semiconductor. This is formally expressed through the *Beer-Lambert-Bouguer* law, which states that the absorbance, A (also called *optical density*), of a medium can be expressed in terms of not just its transmittance: T, relative to a reference: T_0; but also via more fundamental physical parameters related to the media such as an absorption coefficient and thickness [54].

$$A_\lambda = -\log_{10}\frac{T}{T_0} = \varepsilon_\lambda \cdot C \cdot L \qquad (1.4)$$

In a typical absorption measurement as depicted in Figure 1.8, light of several wavelengths is passed through the media which can be either a solution or thin film, and the fraction of light transmitted through it is determined per wavelength yielding a spectrum – usually plotted as absorbance (or absorption coefficient) versus wavelength (or energy). In most cases, we are interested in not only the absorption intensity, but also in the onset - which gives an indication of the bandgap of the medium, and to material-specific features which sometimes shed additional information on certain photophysical processes – examples of these are vibronic progressions in polymers, and excitonic absorption peaks in QDs.

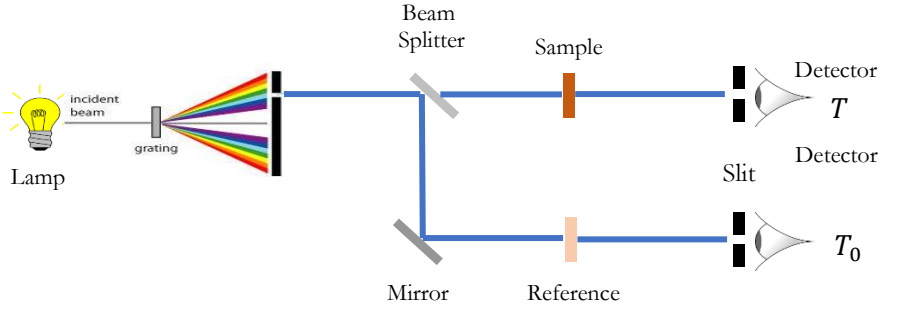

Figure 1.8: Schematic of a dual-beam absorption spectrophotometer.

1.7.2 Photoluminescence Spectroscopy

Photoluminescence (or fluorescence) is a particular case of light emission (luminescence) which occurs upon the absorption of a photon of energy by a semiconductor; which is said to be in the excited state[55]. When a photon is absorbed by a semiconductor, the excess energy can be dissipated either via vibrational modes (vibrational relaxation or internal conversion) and/or by the emission of a photon of lower energy (the *Stokes shift* being the difference between the peak absorption and emission energies[56]). A measure of the photoluminescence efficiency of a semiconductor is its' photoluminescence quantum yield (PL-QY) which is defined as the ratio of photons emitted to photons absorbed. In many recent publications, the case has been made for the link between photovoltaic figures of merit (such as the open circuit voltage) and the luminescence efficiency of the absorber layer[57–59].

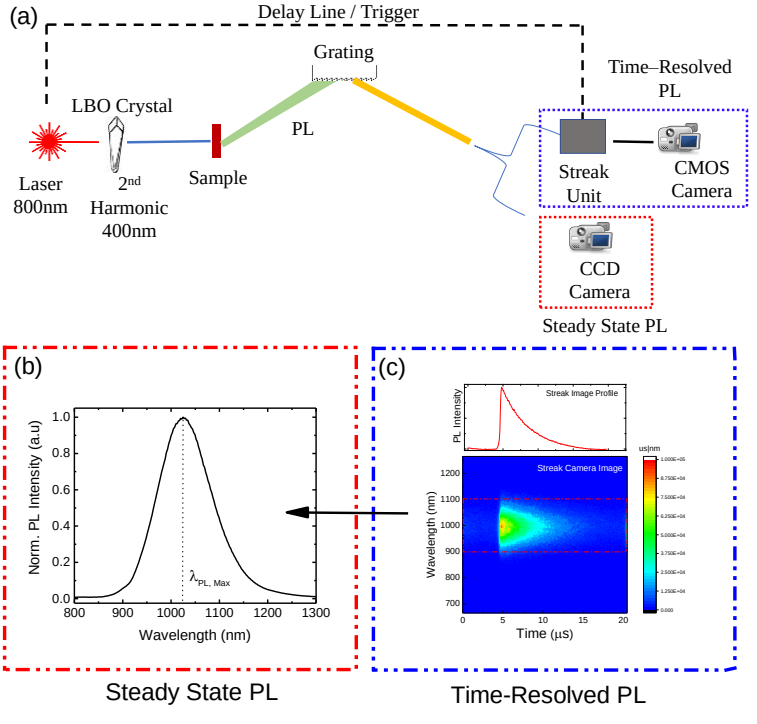

Figure 1.9: (a) the main parts of our "homemade" ultrafast PL spectroscopy setup – for clarity, mirrors and lenses have been omitted (b & c) typical steady-state and time resolved spectra, in this case, they show the PL emission and decay of a PbS QD ink.

In a typical PL spectroscopy experiment depicted in Figure 1.9, a sample is excited with light of higher energy than its' bandgap (non-resonant excitation), with the use of suitable filters, the PL signal is passed through a dispersive element and recorded by a CCD camera. This can be carried out in an instrument called a fluorimeter or more sophisticated "homemade" setups. With the development of ultrafast laser sources, it has also become relatively straightforward to perform measurements of the PL lifetime (or time-resolved PL).

Measuring the dynamics of PL can shed additional information on photophysical processes and aid in the selection and identification of suitable materials for optoelectronic applications. The measurements performed in this thesis were carried out with a homemade setup based on a pulsed Ti:Sapphire laser (pulse width ~ 150 fs, repetition rate 76 MHz) with a spectrometer coupled to CCDs with or without a streak unit; in the former case, steady-state spectra are obtained and in the latter, a so-called streak-image is obtained. A streak image is a 3 dimensional map where light intensity is recorded for every wavelength and delay time. From these maps PL decay profiles or time-resolved PL spectra can be easily extracted.

1.7.3 Solar Cell Current-Voltage Characteristics

A solar cell in the dark is a diode, displaying an extremely low current in reverse bias and a small voltage drop across it under forward bias conditions. Conversely, under illumination, electrical power is produced by charges generated within the active layer which "shifts" the characteristic current versus voltage (I -V) curve from the 1st (Cartesian) quadrant to the 4th, as shown in Figure 1.10.

Within this quadrant, the current when there is no applied bias is called the short circuit current (denoted I_{SC}); and the voltage across the solar cell when the current-density through it is zero is called the open circuit voltage (denoted V_{OC}); worth noting is that at these points there is no electrical power being produced by the solar cell.

During operation, the solar cell generally produces power somewhere in between these two points; with a maximum at a so-called maximum power point (MPP); where the product of the current and voltage is maximised. Next to the I_{SC} and V_{OC} another important metric is the *fill factor* (FF); which is the ratio of the power produced at the MPP to the total power possible for the solar cell to generate (given by the product of I_{SC} and V_{OC}). It is best thought of as a measure of how closely the solar cell approaches the behaviour of an ideal solar cell. In many cases, to enable comparison between different solar cells – current density, J (= I/A), *i.e.* current per unit area, A) is used instead of current.

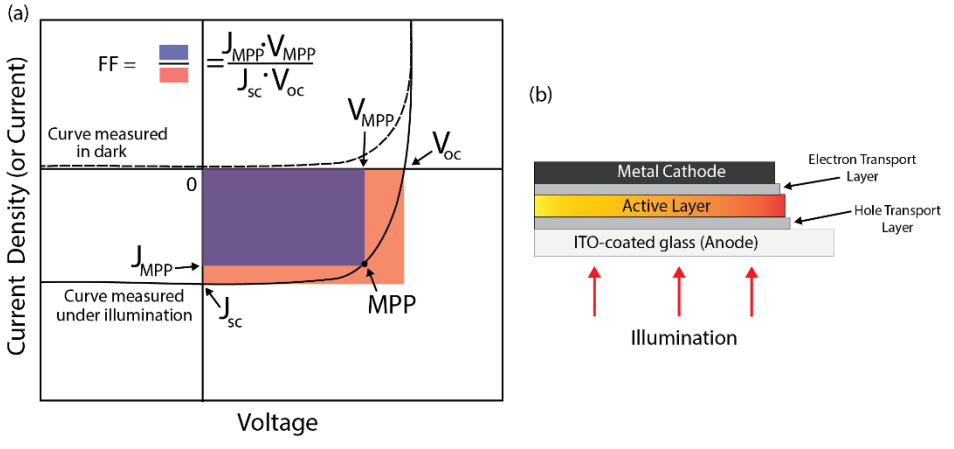

Figure 1.10: (a) a typical *I-V* curve for a solar cell measured under the dark and when illuminated showing the points of interest, and a pictoral representation of the fill factor (b) typical solar cell architecture discussed in this thesis.

A common architecture for solar-cells which feature in this thesis are *p-i-n* junction solar cells, which are similar to *p-n* junction solar cells but with an 'intrinsic' semiconducting layer flanked on both sides by *p*- and *n*- type layers which serve to create an internal electric field which depletes the intrinsic layer causing generated carriers to drift towards the *p*- or *n*- layers. For this reason, the *p*- and *n*- layers are sometimes referred to as charge transport (hole-/electron-) layers.

The power conversion efficiency (PCE) of a solar cell (see equation 1.5) is therefore defined in terms of these quantities under test conditions which require the temperature, light intensity (I) and the spectral distribution of light to be standardised to 25 °C, 1 sun (=1000 W/m^2), and AM1.5G (spectrum of sunlight after passing through an optical path 1.5 times the thickness of earth's atmosphere).

$$PCE = \frac{FF \cdot J_{sc} \cdot V_{oc}}{I} \qquad (1.5)$$

Thus, in device optimisation, the goal is to either maximise the fill-factor, short-circuit current or open-circuit voltage. In practice, because of the complex relationship between these 3 metrics, to maximise the efficiency, they must be simultaneously optimised. In device-centred studies, understanding the charge transport and possible loss mechanisms (trap-assisted or bimolecular recombination) in the active layer of solar cells made from disordered semiconductors is usually performed by light-intensity dependent measurements of the open circuit voltage and closed circuit current[60,61].

1.8 Outline

Chapter 2 deals with an approach of making a 3-component (ternary) blend of a polymer, fullerene derivative and PbS QDs in order to increase the dielectric constant of the blend. The dielectric constant of blends for organic solar cells is believed to be one of several limiting factors to achieving proper exciton dissociation and thus, improved efficiency. Although there have been several prior successful attempts at making ternary OPVs, the predominant goal has always been to improve coverage of the solar irradiance spectrum by incorporating materials with complementary absorption rather than aiming to use the third component as a means to increase the dielectric constant of the blends. In this chapter, we add small amounts of PbS QDs to a blend of a narrow bandgap copolymer and a fullerene derivative and use the photoluminescence of the interfacial charge transfer state as a measure of the local dielectric constant of the blend.

In **chapter 3**, the concept of ferroelectric OPV (FE-OPV) is revisited with the aim of reconciling disparate views in the literature. Therein, a newly synthesized (and previously unreported) semiconducting-ferroelectric block copolymer is used a compatibilizer to overcome the severe phase segregation that often occurs when ferroelectric polymers are mixed with semiconducting ones. Using an optimized deposition recipe, we obtain smooth, pinhole-free ternary blends of semiconducting and ferroelectric components which we use for device fabrication, spectroscopic measurements and poling experiments.

In **chapter 4**, the microstructure and electron extraction layers of perovskite solar cells (PSCs) are studied; with particular emphasis on understanding how they affect light-soaking, and the eventual photovoltaic performance. The light soaking effect is a reversible increase in the performance of perovskite solar cells upon extended illumination, and represents an important barrier to proper functioning perovskite solar cells. In the first part, the deposition recipe of the perovskite is varied to obtain either compact or coarse morphologies for device characterization and spectroscopic measurements; going further, two fullerene derivatives with different dielectric constants are compared as electron transport layers. In both parts, spectroscopic measurements were combined with device characterization to understand the origin of the light soaking effect.

Finally, **chapter 5** reports a detailed photophysical characterization of two different bismuth-perovskite shelled PbS QDs obtained as an ink via a phase transfer ligand exchange process to replace the native oleic acid ligands. Electrical characterization on field effect transistors based on the Bi-perovskite shelled QD solids were performed to show the successful removal of the oleic acid ligands, with the fabricated transistors displaying electron mobilities comparable to reported values for epitaxial Pb-based shelled QDs. Afterward, the optical properties of the inks and solids were studied using a combination of absorption, temperature-, and power-dependent (PL) spectroscopies.

References

[1] United Nations, "Sustainable Develpment Goals," can be found under https://www.un.org/sustainabledevelopment/development-agenda/, **2015**.

[2] United Nations Framework Convention on Climate Change, "The Paris Agreement," can be found under https://unfccc.int/process-and-meetings/the-paris-agreement/the-paris-agreement, **2015**.

[3] Enerdata, *Global Energy Statistical Yearbook*, **2018**.

[4] W. Palz, *Power for the World*, Pan Stanford Pte Ltd, Singapore, **2010**.

[5] W. Shockley, H. J. Queisser, *J. Appl. Phys.* **1961**, *32*, 510.

[6] M. Rubinstein, R. H. Colby, *Polymer Physics*, Oxford University Press, Oxford, **2003**.

[7] H. Shirakawa, E. J. Louis, A. G. MacDiarmid, C. K. Chiang, A. J. Heeger, *Polymer (Guildf).* **1977**, *36*, 578.

[8] Royal Swedish Academy of Sciences, "The Nobel Prize in Chemistry 2000," can be found under https://www.nobelprize.org/prizes/chemistry/2000/press-release/, **2000**.

[9] S. C. Rasmussen, *Bull. Hist. Chem.* **2014**, *39*, 64.

[10] W. Brütting, Ed. , *Physics of Organic Semiconductors*, Wiley-VCH Verlag, Weinheim, **2005**.

[11] K. Fukui, T. Yonezawa, H. Shingu, *J. Chem Phys* **1952**, *20*, 722.

[12] C. A. Coulson, *Coulson's Valence*, Oxford University Press, Oxford, **1979**.

[13] A. Köhler, H. Bässler, *Electronic Processes in Organic Semiconductors*, Wiley-VCH Verlag, Weinheim, **2015**.

[14] G. Lanzani, *The Photophysics behind Photovoltaics and Photonics*, Wiley-VCH Verlag, **2012**.

[15] M. Hiramoto, H. Fujiwara, M. Yokoyama, *J. Appl. Phys.* **1992**, *72*, 3781.

[16] J. J. M. Halls, C. A. Walsh, N. C. Greenham, E. A. Marseglia, R. H. Friend, S. C. Moratti, A. B. Holmes, *Nature* **1995**, *376*, 498.

[17] G. Yu, J. Gao, J. C. Hummelen, F. Wudl, A. J. Heeger, *Science (80-.).* **1995**, *270*, 1789 LP.

[18] M. Manca, C. Piliego, E. Wang, M. R. Andersson, A. Mura, M. a. Loi, *J. Mater. Chem. A* **2013**, *1*, 7321.

[19] M. A. Izquierdo, R. Broer, R. W. A. Havenith, *J. Phys. Chem. A* **2019**, *123*, 1233.

[20] A. Dieckmann, H. Bässler, P. M. Borsenberger, *J. Chem Phys* **1993**, *99*, 8136.

[21] N. W. Ashcroft, N. D. Mermin, *Solid State Physics*, Saunders College Publishing, **1976**.

[22] A. J. Lovinger, *Science (80-.).* **1983**, *220*, 1115.

[23] R. C. G. Naber, J. Massolt, M. Spijkman, K. Asadi, P. W. M. Blom, D. M. De Leeuw, *Appl. Phys. Lett.* **2007**, *90*, 113509.

[24] K. Asadi, P. De Bruyn, P. W. M. Blom, D. M. De Leeuw, *Appl. Phys. Lett.* **2011**, *98*, 183301.

[25] K. S. Nalwa, J. A. Carr, R. C. Mahadevapuram, H. K. Kodali, S. Bose, Y. Chen, J. W. Petrich, B. Ganapathysubramanian, S. Chaudhary, *Energy Environ. Sci.* **2012**, *5*, 7042.

[26] P. Martins, A. C. Lopes, S. Lanceros-Mendez, *Prog. Polym. Sci.* **2014**, 683.

[27] K. Asadi, D. M. De Leeuw, B. De Boer, P. W. M. Blom, *Nat. Mater.* **2008**, *7*, 547.

[28] A. G. Shulga, V. Derenskyi, J. M. Salazar-Rios, D. N. Dirin, M. Fritsch, M. V Kovalenko, U. Scherf, M. A. Loi, *Adv. Mater.* **2017**, *1701764*, 1.

[29] A. P. Alivisatos, *Science (80-.).* **1996**, *271*, 933.

[30] D. Vanmaekelbergh, P. Liljeroth, *Chem. Soc. Rev.* **2005**, *34*, 299.

[31] L. E. Brus, *J. Chem. Phys.* **1984**, *80*, 4403.

[32] X. Lan, O. Voznyy, A. Kiani, F. P. García De Arquer, A. S. Abbas, G. H. Kim, M. Liu, Z. Yang, G. Walters, J. Xu, M. Yuan, Z. Ning, F. Fan, P. Kanjanaboos, I. Kramer, D. Zhitomirsky, P. Lee, A. Perelgut, S. Hoogland, E. H. Sargent, *Adv. Mater.* **2016**, *28*, 299.

[33] F. W. Wise, *Acc. Chem. Res.* **2000**, *33*, 773.

[34] R. E. Chandler, A. J. Houtepen, J. Nelson, D. Vanmaekelbergh, *Phys. Rev. B - Condens. Matter Mater. Phys.* **2007**, *75*, 1.

[35] P. R. Brown, D. Kim, R. R. Lunt, N. Zhao, M. G. Bawendi, J. C. Grossman, V. Bulović, *ACS Nano* **2014**, *8*, 5863.

[36] J. Gao, J. C. Johnson, *ACS Nano* **2012**, *6*, 3292.

[37] S. Z. Bisri, E. Degoli, N. Spallanzani, G. Krishnan, B. J. Kooi, C. Ghica, M. Yarema, W. Heiss, O. Pulci, S. Ossicini, M. A. Loi, *Adv. Mater.* **2014**, *26*, 5639.

[38] Y. Cao, A. Stavrinadis, T. Lasanta, D. So, G. Konstantatos, *Nat. Energy* **2016**, *1*, 16035.

[39] M. A. Loi, J. C. Hummelen, *Nat Mater* **2013**, *12*, 1087.

[40] V. M. Goldschmidt, *Naturwissenschaften* **1926**, *14*, 477.

[41] A. Kojima, K. Teshima, Y. Shirai, T. Miyasaka, *J. Am. Chem. Soc.* **2009**, *131*, 6050.

[42] H.-S. Kim, A. Hagfeldt, N.-G. Park, *Chem. Commun.* **2019**, *55*, 1192.

[43] W.-J. Yin, T. Shi, Y. Yan, *Appl. Phys. Lett.* **2014**, *104*, 63903.

[44] K. X. Steirer, P. Schulz, G. Teeter, V. Stevanovic, M. Yang, K. Zhu, J. J. Berry, *ACS Energy Lett.* **2016**, *1*, 360.

[45] J. Liang, C. Wang, Y. Wang, Z. Xu, Z. Lu, Y. Ma, H. Zhu, Y. Hu, C. Xiao, X. Yi, G. Zhu, H. Lv, L. Ma, T. Chen, Z. Tie, Z. Jin, J. Liu, *J. Am. Chem. Soc.* **2016**, *138*, 15829.

[46] M. Saliba, T. Matsui, K. Domanski, J.-Y. Seo, A. Ummadisingu, S. M. Zakeeruddin, J.-P. Correa-Baena, W. R. Tress, A. Abate, A. Hagfeldt, M. Grätzel, *Science (80-.).* **2016**, *354*, 206 LP.

[47] National Renewable Energy Laboratories (NREL), "Best Research Cell Efficiencies," can be found under https://www.nrel.gov/pv/assets/pdfs/pv-efficiency-chart.201812171.pdf, **2018**.

[48] J. Franck, E. G. Dymond, *Trans. Faraday Soc.* **1926**, *21*, 536.

[49] E. Condon, *Phys. Rev.* **1926**, *28*, 1182.

[50] M. Kasha, *Discuss. Faraday Soc.* **1950**, *9*, 14.

[51] J. W. Verhoeven, *Pure Appl. Chem.* **1996**, *68*, 2223.

[52] A. Jablonski, *Nature* **1933**, *131*, 839.

[53] P. W. Atkins, J. De Paula, *Atkins' Physical Chemistry*, Oxford University Press, Oxford ; SE - Xxx, 1064 Pages : Color Illustrations ; 28 Cm, **2006**.

[54] K. Laqua, W. Melhuish, M. Zander, *Pure Appl. Chem.* **1988**, *60*, 1449.

[55] J. R. Lakowicz, *Principles of Fluorescence Spectroscopy*, Kluwer Academic / Plenum, New York, **1999**.

[56] J. R. Albani, *Structure and Dynamics of Macromolecules: Absorption and Fluorescence Studies*, Elsevier Science, Amsterdam, **2004**.

[57] U. Rau, *Phys. Rev. B - Condens. Matter Mater. Phys.* **2007**, *76*, 1.

[58] K. Vandewal, K. Tvingstedt, A. Gadisa, O. Inganäs, J. V. Manca, *Nat. Mater.* **2009**, *8*, 904.

[59] K. Tvingstedt, O. Malinkiewicz, A. Baumann, C. Deibel, H. J. Snaith, V. Dyakonov, H. J. Bolink, *Sci. Rep.* **2014**, *4*, 1.

[60] M. M. Mandoc, F. B. Kooistra, J. C. Hummelen, B. de Boer, P. W. M. Blom, *Appl. Phys. Lett.* **2007**, *91*, 263505.

[61] M. Kuik, L. J. A. Koster, G. A. H. Wetzelaer, P. W. M. Blom, *Phys. Rev. Lett.* **2011**, *107*, 1.

[62] C. Eames, J. M. Frost, P. R. F. Barnes, B. C. O'Regan, A. Walsh, M. S. Islam, *Nat. Commun.* **2015**, *6*, 2.